



Method of Aerial Imaging Multi-Zone Data Complex Processing for Hydrocarbons Remote Exploration

Alexey O. Kovalev

Center for Science Intensive Technologies, Moscow. OJSC CST

Summary

This paper introduces an aerial imaging and multi-zone data processing technology, referred to as CST, that captures differences in spectral emissions at surface as a result of the macro and micro-seepage of hydrocarbons to identify the presence of hydrocarbons. To illustrate the sequence of processing, the paper uses as a control, information from territory with a proven presence of hydrocarbons. Also included is a synopsis of the theory behind the system. This system has been proven over 8 years and on over 30 license blocks.

Introduction

Biological and geochemical processes caused by the macro and micro-seepage of hydrocarbons (HC) lead to spectral signature changes at surface, of soils, minerals and vegetation in different bands of the spectrum. These spectral alterations can be registered by remote imaging (aerial, satellite) and ground based detection methods making it possible to analyse wide-area territories (*References 1-7*).

Some challenges of the existing HC exploration methods include an absence of complex data analysis, both in visual and multiple infrared bands, the use of low quality satellite images to identify low-contrast anomalies, the “dot-grid” structure of land based exploration, an absence of brightness normalization of adjacent images and a disregard of information from neighboring areas in favor of remote (satellite or aerial) methods that combine perhaps a single ground-based geochemical or geophysical survey.

The aim of CST technology is to improve the present methods to delineate the HC anomalies through the coordinated integration of multiple spectral features as identified in aerially captured images.

Theory and Method

Phase 1

Step 1 - Conduct a review of the geographic and geological features of the target area and the areas in the immediate vicinity. The planning of aerial imaging capture is also undertaken.

Step 2 - Conduct the aerial image and coordinate capture using specialist scanners. Image collection is preferably conducted in a single session and by overlapping profiles (captured in a linear manner along the line of flight) and with a spatial resolution of 7-10 m. At least one of the routes must cover an area with a proven HC presence for calibration and control purposes.

Step 3 - Primary processing of information includes standard procedures for the removal of radiometric distortions, brightness correction, impulse noise filtering, geometric correction, routes stitching and pixel coordinate correlation.

Registered digital images $I_{\lambda_j}(m, n)$,

where I – pixel (m,n) brightness, λ - spectrum band number, j - route number,

are processed in proprietary software. Daytime images of all planned spectral bands and night images of thermal bands are processed in a similar manner. An image of every profile, in every spectral band, is corrected for brightness and the ‘inter-profile’ brightness difference is removed. According to navigation information, reference coordinate points and scanning parameters, geometry distortions are also corrected. Geometry corrected images of all routes $I_{\lambda j}(m,n)$ are transformed to a cartographic projection and unified into a single mosaic image $D_{\lambda}(x,y)$,

where D_{λ} – brightness code of (x,y) pixel of mosaic image in the λ -th spectrum band.

The result of this primary processing phase is the creation of images in a set of spectral bands for further thematic mapping.

Phase 2

The second phase of data processing utilizes proprietary algorithms for the detection of specific HC influenced anomalies. Biological and geochemical processes as a result of HC seepage cause changes in spectral, and consequently reflectance and brightness, characteristics at surface (soils, vegetation). These are in contrast to similar objects not in direct proximity of HC deposits (*References 1-7*). To detect low contrasts on mosaic images, caused by HC anomalies, the images are processed according to a set of parameters obtained from analysis of the reference area.

The images of the target area are then delineated and referenced $D_{\lambda}(x,y)$. For each delineated area a histogram of pixel brightness distribution for each spectral band with noise sampling cutoffs is then created. The Pixel Brightness Band is then calculated $D_{\lambda,\min} \div D_{\lambda,\max}$ and all spectral bands images normalized for brightness.

$$D_{\lambda}^*(x,y) = \begin{cases} 0, & D_{\lambda}(x,y) < D_{\lambda,\min} \\ \frac{D_{\lambda}(x,y) - D_{\lambda,\min}}{D_{\lambda,\max} - D_{\lambda,\min}} \cdot 1024, & D_{\lambda,\min} \leq D_{\lambda}(x,y) \leq D_{\lambda,\max} \\ 1024, & D_{\lambda}(x,y) > D_{\lambda,\max} \end{cases}$$

where $D_{\lambda}^*(x,y)$ ($\lambda = \overline{1, N}$, N - number of considered spectral bands)

– images normalized for brightness of visual and thermal spectrum bands.

Every normalized image $D_{\lambda}^*(x,y)$ ($\lambda = \overline{1, N}$) underwent low-pass filtering to remove noise and to obtain uniform brightness areas

$$\hat{D}_{\lambda}(x,y) = D_{\lambda}^*(x,y) \otimes H,$$

(\otimes - image convolution operator with Gauss filter mask H).

Filtered images then undergo a threshold binarization procedure,

$$S_{\lambda}(x,y) = \begin{cases} 1, & \hat{D}_{\lambda,\min}(x,y) \leq \hat{D}_{\lambda}(x,y) \leq \hat{D}_{\lambda,\max}(x,y) \\ 0, & \text{otherwise} \end{cases}$$

where $S_{\lambda}(x,y)$ - binary image, $\hat{D}_{\lambda,\min}(x,y)$, $\hat{D}_{\lambda,\max}(x,y)$ - binarization thresholds are calculated by delineated areas on the basis of filtered images $\hat{D}_{\lambda}(x,y)$.

As a result of binarization, a brightness code will be assigned to pixels with the same brightness characteristics as pixels of delineated areas.

In practice it is possible that the reflectance characteristics of surface objects that have undergone biological and geochemical transformations as a result of HC influence, will be similar or the same as other non-influenced objects. This will result in the creation of 'false positives' on the binarized images $S_{\lambda}(x, y)$. Such instances are both rare and will be clearly identifiable when considered under different spectral bands. For example, a false temperature anomaly detected in 8.0-14 μm would not be detectable in a 0.43-0.49 μm image. So in order to improve the reliability one combines multiple spectral band binarized images (similar to Fig. 1).

$$S(x, y) = \sum_{\lambda=1}^N S_{\lambda}(x, y),$$

where $S(x, y)$ – grayscale image of explored area.

On the image $S(x, y)$ areas with a maximum value of signal S have the greatest likelihood of corresponding to HC anomalies. These areas are plotted on to a map for further matching with other existing data. For improved visual control, the image $S(x, y)$ is inverted by brightness. An example of an inverted image is represented in Fig. 1.

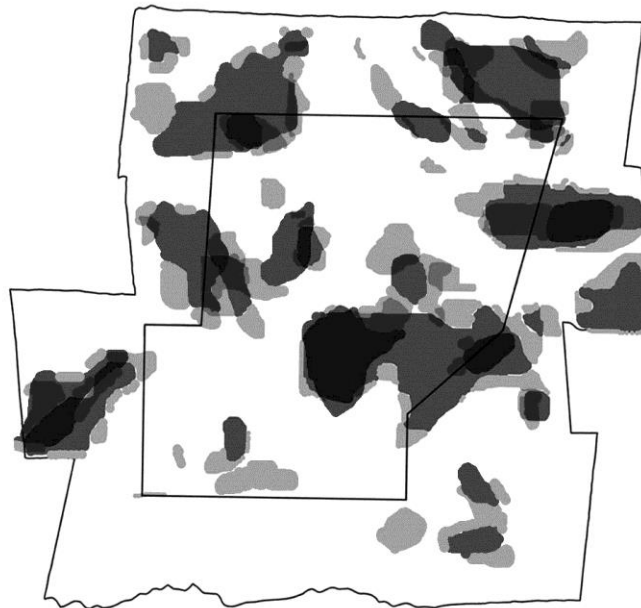


Fig 1. Example of a Combined Spatial and Brightness-inversion image.

Here the darkest areas of the image correspond to presumed HC anomalies (maximum S value), white color areas have no prospects for exploration, light gray areas represent 'false-delineated' areas.

The anomalies are then linked to geodesy coordinates and represented in the proprietary software's geoinformation system and can be integrated with any other geological analysis and used to support the planning of further exploration, including drilling.

Examples

This technology has been successfully trialed and used on licensed blocks from 2005-2013. The majority of the work has been performed in Western Siberia (Khanty-Mansiysky Autonomous District, Tumen region, Omsk region). The processed data has been compared, with results showing a high

correspondence, against ground-based findings in the Schuchy and Mlechny licensed blocks, over the 8 year period.

Conclusions

Correlation of the results obtained over 8 years and on over 30 licensed blocks confirms the stability of the CST identified HC anomalies over time, the efficiency of the detection algorithm and the robustness of the delineation approach to accidental factors such as current year weather conditions, biomass state, humidity and other parameters of soil, solar radiation and atmospheric condition while imaging.

References

- [1] *Balabayev D., Hutchison P., Tomin G.* Surface footprints of the hydrocarbon trap as revealed by RSDD-H Exploration Mapping. Scotforth Limited, 2010. – <http://www.scotforth.com> (13.11.2010).
- [2] *Gupta P., Chakraborty R., Awasthi A.* Model thermal anomalies over petroliferous basins // *Oil & Gas Journal.* – 2010, – Vol. 108. – N 28. – pp. 72-75.
- [3] *Lloyd F.* Finding, mapping temperature anomalies can aid oil, gas exploration // *Oil & Gas Journal.* – 2001, – Vol. 99, N 23. – pp.38-48.
- [4] *Thenkabail P.S., Smith R.B., De Pauw E.* Evaluation of Narrowband and Broadband Vegetation Indices for Determining Optimal Hyperspectral Wavebands for Agricultural Crop Characterization // *Photogrammetric Engineering & Remote Sensing.* – Vol. 68. – N 6. – 2002. – pp. 607-621.
- [5] *Yang H.* Spectral characteristics of wheat associated with hydrocarbon microseepages, // *International Journal of remote sensing.* – Vol 20.– Issue 4. –1999. – pp.807-813.
- [6] *Nooman M.F.* Hyperspectral reflectance of vegetation affected by underground hydrocarbon gas seepage, // ISBN: 978-90-8504-671-4, International Institute for Geo-information Science and Earth Observation, Enschede, the Netherlands, 2007, ITC Dissertation number :145.
- [7] *McCoy, R.M., Blake, J.G., Andrews, K.L.,* "Detecting hydrocarbon microseepage using hydrocarbon absorption band of reflectance spectra of surface soils," // *Oil & Gas Journal.* – 2001, – Vol. 99, N 22 – pp. 40-45.